Layers of Close-Packed Alternated Enantiomorphous Helices and the Three Different Uniplanar Orientations of Syndiotactic Polystyrene

Alexandra R. Albunia,*,‡ Paola Rizzo,‡ Oreste Tarallo,† Vittorio Petraccone,† and Gaetano Guerra‡

Dipartimento di Chimica and INSTM Research Unit, Università degli Studi di Salerno, Via Ponte don Melillo, 84084, Fisciano, Italy, Dipartimento di Chimica "Paolo Corradini", Università di Napoli "Federico II", Complesso di Monte S. Angelo, via Cintia, 80126 Napoli, Italy

Received May 27, 2008; Revised Manuscript Received September 5, 2008

ABSTRACT: Thorough analyses of X-ray diffraction patterns of syndiotactic polystyrene (s-PS) films, exhibiting different crystalline and co-crystalline phases, and related evaluations of degrees of orientation have allowed to give a more accurate as well as simpler description of the three known uniplanar orientations. This new description involves the three simplest orientations of the high density *ac* layers (i.e. of the layers of close-packed alternated enantiomorphous s-PS helices) with respect to the film plane. On this basis it is proposed that the three uniplanar orientations should be named $a_{\parallel}c_{\parallel}$, $a_{\parallel}c_{\perp}$ and $a_{\perp}c_{\parallel}$, i.e., by a nomenclature which also presents the advantage to be independent of the helical crystalline or co-crystalline s-PS phase.

Introduction

Two crystalline phases of syndiotactic polystyrene (s-PS), i.e. the deeply studied δ phase[1] and the recently discovered ε phase,[2] constitute the first examples of polymeric frameworks, i.e. of polymeric crystalline phases with a density lower than the corresponding amorphous phase and with empty space distributed as isolated cavities and channels, respectively. Materials (mainly films[3] and aerogels[4]) presenting these nanoporous s-PS phases are promising for applications in chemical separations (mainly air/water purification) as well as in sensorics.[5]

Starting from these nanoporous phases, as well as by suitable solution crystallization procedures, co-crystalline phases of s-PS with a large number of low-molecular-mass guest molecules can be easily obtained. In most cases *clathrate* phases, including isolated guest molecules (generally one per cavity, corresponding to a maximum molar ratio guest/host-monomer-unit of 1/4),[6] are formed while in few cases *intercalate* phases, including layers of guest molecules intercalated with layers of polymer helices (corresponding to maximum molar ratio guest/host-monomer-unit of 1/2), are obtained.[7] In this respect it is worth noting that films presenting s-PS/active-guest co-crystalline phases have been proposed as advanced materials, mainly for optical applications (e.g., as fluorescent, photo-reactive and chromophore materials).[8]

The monoclinic nanoporous δ phase[1] and all the corresponding co-crystalline phases with low molecular mass guests,[6,7] exhibit a common structural feature, i.e. layers of close-packed alternated enantiomorphous s(2/1)2 helices (Figure 1).

The distance between the helical axes in these layers (0.87 nm) remains essentially unaltered for all co-crystalline phases and as a consequence their *a* axis is poorly dependent on the chemical nature of the guest, i.e. nearly double of this interchain distance (1.74 ± 0.02 nm). As usual for crystalline phases with a same polymer conformation, also the *c* periodicity (0.78 ± 0.01 nm) along the chain axis remains essentially constant. As a consequence the layers of Figure 1 can be described as *ac* layers and the crystalline structures of the nanoporous δ phase

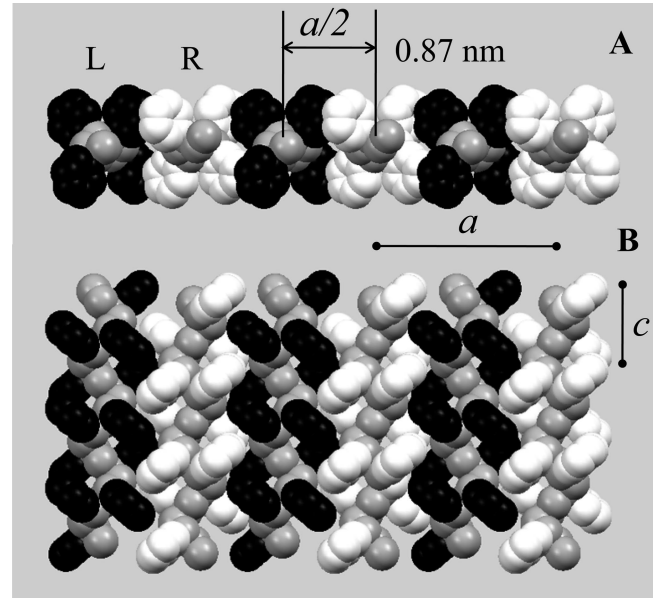

Figure 1. Top (A) and lateral (B) views of the layer of s(2/1)2 parallel helices of s-PS, i.e. the high density and low-energy structural feature which is common to the δ nanoporous form and to the corresponding co-crystalline (both clathrate and intercalate) forms. The minimum interchain distance (0.87 nm) is achieved by alternating enantiomorphous helices (R and L stand for right-handed and left-handed, respectively).

and of the derived co-crystalline phases substantially differ only in the *b* crystalline axis and in the γ angle (between *a* and *b* axes). On this basis, all s-PS co-crystalline phases, which by guest removal can be transformed in the nanoporous δ phase, can be simply described in terms of *ac* interlayer distance, i.e., in terms of the distance between layer of close-packed enantiomorphous helices.[7d] In fact, this distance, which for the δ form phase is equal to 1.05 nm, can increase depending on the guest volume up to nearly 1.2 nm for clathrate co-crystals while ranges from 1.3 up to 1.8 nm for the known intercalate co-crystals.[7d]

Recent studies have shown that suitable processing conditions can lead to the unprecedented formation of co-crystalline films exhibiting three different kinds of uniplanar orientations of the

* Corresponding author. Telephone: +39 (0) 89 969392. Fax: +39 (0) 89 969603. E-mail: aalbunia@unisa.it.
† Dipartimento di Chimica "Paolo Corradini", Università di Napoli "Federico II".
‡ Dipartimento di Chimica and INSTM Research Unit, Università degli Studi di Salerno.

10.1021/ma801180b CCC: $40.75 © 2008 American Chemical Society
Published on Web 10/29/2008

co-crystalline phases.[9−11] The degree and the kind of uniplanar orientation depends on the selected technique (solution crystallization procedures[9] or solvent induced crystallization in amorphous samples[10] or solvent induced re-crystallizations of γ and α unoriented samples[11]) as well as on the chemical nature of the guest. It is worth noting that high degrees of uniplanar orientations have been obtained for very broad film thickness ranges (at least from 100 nm up to 200 μm).[9a,10a−c] The three uniplanar orientations (without substantial loss of their degree of orientation) are maintained not only for the δ phase, as obtained by suitable guest-removal procedures, but also for the γ phase[12] as obtained by suitable thermal treatments.[10b,c] The three uniplanar orientations can be also maintained[10b,c] after guest-exchange procedures transforming the co-crystalline s-PS phase with a given guest into a co-crystalline phase with a different guest.[13]

The three kinds of uniplanar orientations have been described, for the δ phase as (010),[9a] (002),[9b,10b] or ($\bar{2}$10)[10c] while for the γ phase as (020),[9a] (002),[10b] or (200),[10c] respectively, thus indicating that these crystalline planes are preferentially oriented parallel to the film plane.

It is worth adding that suitable thermal treatments on s-PS films presenting the three different *uniplanar* orientations of their helical crystalline phases can lead to films with *planar* orientations of their zig-zag planar α[14] and β[15] crystalline phases (by annealing up to 250 °C).[9a,10b] In particular, films with (00*l*) and (*hk*0) orientations lead to crystalline phases with their chain axes preferentially perpendicular and parallel to the film surface, respectively.[10c]

The availability of s-PS films with three different kinds of uniplanar orientation not only allows to establish fine structural features of s-PS crystalline and co-crystalline phases (e.g., experimental evaluation of the orientation of transition moment vectors of host and guest vibrational modes, with respect to the host chain axes)[16] but can be relevant also for practical purposes. For instance, it allows guest orientation control[17] for co-crystalline phases and guest diffusivity (and hence permeability) control[18] for the nanoporous phases.

In this paper, on the basis of thorough X-ray diffraction measurements, on different crystalline and co-crystalline phases of s-PS films, and related evaluations of degrees of uniplanar orientation we present a more accurate as well as simpler description of the three observed uniplanar orientations. This new description involves the three simplest orientations of the high planar-density *ac* layers of Figure 1 with respect to the film plane.

Experimental Section

Materials and Preparation Procedures. The s-PS used in this study was manufactured by Dow Chemical Company under the trademark Questra 101. The ^{13}C nuclear magnetic resonance characterization showed that the content of syndiotactic triads was over 98%. The weight-average molar mass obtained by gel permeation chromatography (GPC) in trichlorobenzene at 135 °C was found to be $M_w = 3.2 \times 10^5$ with the polydispersity index, $M_w/M_n = 3.9$.

Pure solvents were purchased from Aldrich and used without further purification.

Co-crystalline films, having a thickness of 25−40 μm, with the (010) uniplanar orientation, i.e., with the *ac* planes preferentially parallel to the film surface ($a_{||}c_{||}$), were obtained by casting procedure from 1% w/w solution in chloroform at room temperature. Co-crystalline films, having a thickness of 100−150 μm, with the other two kinds of uniplanar orientation were obtained by annealing amorphous s-PS films at 200°C for one hour (thus obtaining the α crystalline phase) followed by immersion in suitable solvents for one day at room temperature.[11] In particular, films with the (002) uniplanar orientation, i.e., with the *a* axis preferentially parallel and the *c* axis preferentially perpendicular to the film surface ($a_{||}c_{\perp}$), were obtained by immersion in pure trichloroethylene, while films with the *a* axis preferentially perpendicular and *c* axis preferentially parallel to the film surface ($a_{\perp}c_{||}$) were obtained by immersion in pure chloroform.[11] The amorphous s-PS films were obtained by melt extrusion with an extrusion head of 200 mm × 0.5 mm.

Co-crystalline powders were obtained by treatment of milled pellets in boiling THF for 2 hours.

Unoriented and oriented samples, exhibiting the nanoporous δ phase, were obtained from the s-PS co-crystalline samples by immersion in acetonitrile for 3 hours. In all cases, 100 minutes of desorption at room temperature were sufficient to remove the acetonitrile. The residual guest content in the samples, after these extraction procedures, as evaluated by thermogravimetric measurements, was lower than 0.1%.

Most s-PS/DMNP intercalate samples (powders and $a_{||}c_{||}$ and $a_{||}c_{\perp}$ films) were obtained by immersion of the corresponding nanoporous δ form samples in DMNP for one day, generally at room temperature and at 50°C for the films with $a_{||}c_{\perp}$ uniplanar orientation. Films with $a_{\perp}c_{||}$ uniplanar orientation of the s-PS/DMNP intercalate phase were obtained by immersion of amorphous films in DMNP for one day at room temperature.

Unoriented and oriented s-PS γ form samples were obtained by annealing of the corresponding nanoporous δ form samples at 160 °C for 2 h.

All the considered samples are semi-crystalline with degree of crystallinity in the range 30−45%, as determined by the Fourier transform infrared method described in ref 19.

Characterization Techniques. Wide-angle X-ray diffraction patterns with nickel filtered CuKα radiation were obtained, in reflection, with an automatic Bruker diffractometer. Wide-angle X-ray diffraction patterns were also obtained, in transmission, by using a cylindrical camera (radius = 57.3 mm). In the latter case the patterns were recorded on a BAS-MS imaging plate (FUJIFILM) and processed with a digital imaging reader (FUJIBAS 1800). In particular, to recognize the kind of crystalline phase orientation, photographic X-ray diffraction patterns were taken by having the X-ray beam parallel (EDGE) and perpendicular (THROUGH) to the film surface and by placing the film sample parallel to the axis of the cylindrical camera.

Definition of Degree of Orientation of a Crystal Plane with Respect to the Film Plane. The degree of orientation of a crystal plane exhibiting *hkl* Miller indexes (f_{hkl}), with respect to the film plane, has been formalized on a quantitative numerical basis, in analogy with the Hermans' orientation functions as defined for the axial orientation in refs.:[20]

$$f_{hkl} = (3\overline{\cos^2 x_{hkl}} - 1)/2 \quad (1)$$

by assuming $\overline{\cos^2 x_{hkl}}$ as the average cosine squared values of the angle, x_{hkl}, between the normal to the film surface and the normal to the (*hkl*) crystallographic plane.

If the direction normal to the *hkl* plane is unique (i.e., there are no other equivalent directions in the crystal),[20a] f_{hkl} is equal to +1 or −0.5 when the (*hkl*) crystallographic planes of all crystallites are perfectly parallel or perpendicular to the film plane, respectively. For the case of random orientation f_{hkl} is equal to zero. In this respect it is worth adding that all directions normal to *hkl* planes considered in this paper are unique (see Table I of ref 20a).

The quantity $\overline{\cos^2 x_{hkl}}$ has been experimentally evaluated, by the above-described EDGE X-ray diffraction patterns, as

$$\overline{\cos^2 x_{hkl}} = \overline{\cos^2 \chi_{hkl}} = \frac{\int_0^{\pi/2} I(\chi_{hkl}) \cos^2 \chi_{hkl} \sin \chi_{hkl} \, d\chi_{hkl}}{\int_0^{\pi/2} I(\chi_{hkl}) \sin \chi_{hkl} \, d\chi_{hkl}} \quad (2)$$

where $I(\chi_{hkl})$ is the intensity distribution of a (*hkl*) diffraction on the Debye ring and χ_{hkl} are the azimuthal angles measured from the horizontal lines of EDGE patterns like those of Figures 2 and 3 [In this respect it is worth recalling that the reference directions for samples presenting axial and uniplanar orientation are the

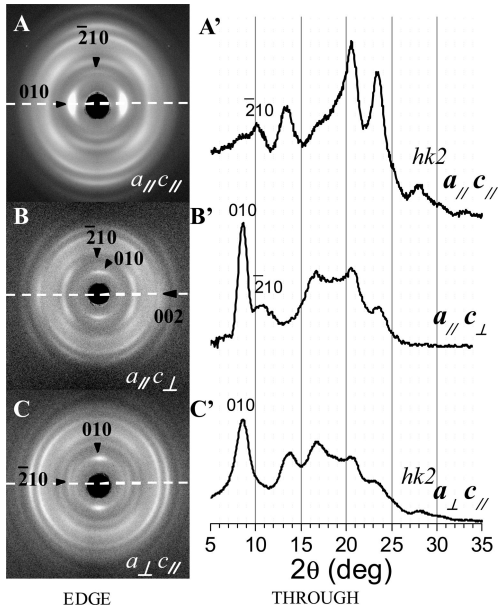

Figure 2. X-ray diffraction patterns of three s-PS films, presenting different kinds of uniplanar orientation of the nanoporous δ crystalline phase.[9,10] (A−C) Photographic patterns taken with X-ray beam parallel to the film surface (EDGE patterns). (A′−C′) Diffraction profiles of photographic patterns taken with X-ray beam perpendicular to the film surface (THROUGH patterns). The three orientations can be defined as $a_{||}c_{||}$, $a_{||}c_{\perp}$ and $a_{\perp}c_{||}$ uniplanar and described by the molecular models of Figure 4A−C, respectively. In parts A−C, dashed horizontal lines indicate the direction normal to the film plane and hence the reference line from which the χ angles have been measured.

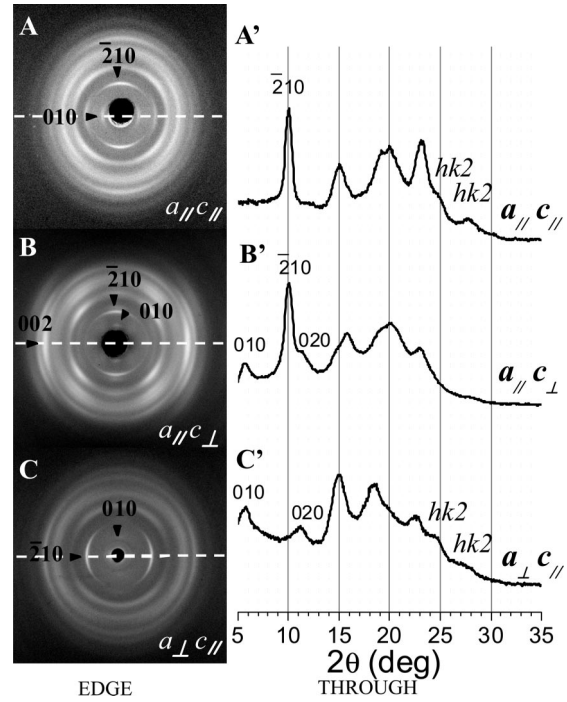

Figure 3. X-ray diffraction patterns of three s-PS films, presenting different kinds of uniplanar orientation of the intercalate co-crystalline phase with DMNP.[9,10] (A−C) Photographic patterns taken with X-ray beam parallel to the film surface (EDGE patterns). (A′−C′) Diffraction profiles of photographic patterns taken with X-ray beam perpendicular to the film surface (THROUGH patterns). The three orientations can be defined as $a_{||}$ $c_{||}$, $a_{||}$ $c_{\perp}$ and $a_{\perp}$ $c_{||}$ uniplanar and described by molecular models analogous to those of Figure 4A−C, respectively. In parts A−C, dashed horizontal lines indicate the direction normal to the film plane and hence the reference line from which χ angles have been measured.

drawing direction and the normal to the film plane, respectively. As for the X-ray diffraction patterns, for the case of axial orientation, the **reference direction** (drawing axis) is generally **parallel** to the axis of the cylindrical camera. On the other hand, for the case of EDGE patterns of films with uniplanar orientation is much more practical to mount the film with its plane parallel to the axis of the cylindrical camera, and as a consequence the **reference direction** (the normal to the film plane) is **perpendicular** to the axis of the camera. As a consequence, the reference direction is horizontal in X-ray diffraction patterns like those of Figures 2 and 3.]

In particular, the diffracted intensity $I(\chi_{hkl})$ of eq 2 has been obtained from EDGE patterns as collected by using a flat camera, recorded on a BAS-MS imaging plate (FUJIFILM) and processed with a digital imaging reader (FUJIBAS 1800), by the azimuthal profile at a constant 2θ value.

Calculation Methods of Diffraction Patterns. Calculated X-ray diffraction patterns (Edge and THROUGH) of simulated samples of s-PS δ form presenting the three uniplanar orientations described before ($a_{||}c_{||}$, $a_{||}c_{\perp}$, and $a_{\perp}c_{||}$) have been carried out using commercially available software (*Cerius*[2] version 4.2 by Accelrys Inc., *Diffraction crystal—fiber diffraction module*). These calculations have been performed using the structural model proposed in ref 1a but changing the proposed monoclinic cell with a new one, nearly orthorhombic, compatible with the lattice of the previous one and assuming a P1 symmetry. The new cell parameters are as follows: $a = 1.74$ nm and $c = 0.77$ nm (equals those reported in literature), $b = 3.17$ nm and $\gamma = 87.72°$. Its content corresponds to three times that of the monoclinic cell. The new cell allowed calculating in a simple way flat plate fiber X-ray diffraction patterns of films presenting the three uniplanar orientation by placing a (for the case $a_{\perp}c_{||}$), b (for the case $a_{||}c_{||}$), or c (for the case $a_{||}c_{\perp}$) axis perpendicular to the film plane. This fact let us to orient the ac layer of the crystal structure of the s-PS δ form in the three simple ways suggested before. Calculated EDGE and THROUGH fiber diffraction patterns were obtained by assuming the fiber axis (normal to the film plane and coincident with a or b or c axis of the new cell) respectively perpendicular and parallel to the X-ray beam. Different parameters have been used in order to better reproduce the experimental X-ray diffraction patterns. In the case of Figure 6A−C, the crystallite dimensions have been taken as 200 Å along a and b while being 100 Å along c. $a = b = 500$ Å and $c = 100$ Å have been used for the case of Figure 6A′−C′ while $a = b = 100$ Å and $c = 80$ Å have been used for the case of Figure 6A″−C″. An orientation degree of the a, b, and c axes in respect to the normal to the film plane has been introduced by an orientation factor specifying the half-width at half-height of crystallite orientation distribution (taken to be a Gaussian centered on the fiber axis). This factor was assumed 10 for the cases of Figure 6, parts A−C, A′−C′, and A″, 15 for the case of Figure 6B″ and 20 for the case of Figure 6C″. The indexes (hkl) reported in Figure 6 are given according to the monoclinic unit cell of ref 1a.

The calculated azimuthal angles (χ_{calcd}) reported in Tables 1 and 2 were determined by using eqs 3, 4, and 5 for $a_{||}c_{||}$, $a_{||}c_{\perp}$, and $a_{\perp}c_{||}$ uniplanar orientations, respectively:

$$\chi_{hkl}(a_{||}c_{||}) = \arccos\left(d_{hkl}\left|h\frac{\cos\gamma}{a\ sen\gamma} - k\frac{1}{b\ sen\gamma}\right|\right) \quad (3)$$

$$\chi_{hkl}(a_{||}c_{\perp}) = \arccos\left(d_{hkl}\frac{l}{c}\right) \quad (4)$$

$$\chi_{hkl}(a_{\perp}c_{||}) = \arccos\left(d_{hkl}\frac{|h|}{a}\right) \quad (5)$$

Results and Discussion

X-ray Diffraction Patterns Taken with Beam Parallel or Perpendicular to the Surface of Films Presenting Uniplanar Orientations of Their Crystalline Phases. X-ray diffraction patterns of s-PS films presenting the nanoporous δ crystalline phase and the intercalate co-crystalline phase with

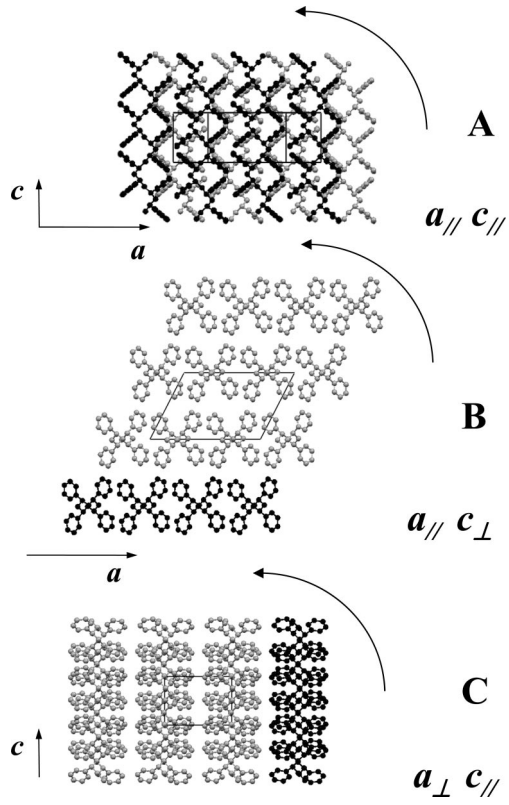

Figure 4. Molecular models showing the three simplest orientations of the layers of alternated enantiomorphous helices of Figure 1 (pointed out by the black color) with respect to the film surface. The plane of the figure is assumed as parallel to the film plane. Arrows in the figures indicate the absence of axial orientation. These three uniplanar orientations can be achieved for γ, δ and most co-crystalline phases of s-PS.

1,4-dimethyl-naphthalene (DMNP), as obtained by a casting procedure from chloroform solution followed by guest removal and by DMNP sorption, are shown in Figures 2, parts A, A′, and 3, parts A, A′, respectively. In particular, the EDGE patterns, i.e. photographic patterns taken with X-ray beam parallel to the film surface, present intense (010) reflections on the equatorial line (Figures 2A and 3A). On the other hand, the THROUGH patterns, i.e. photographic patterns taken with X-ray beam perpendicular to the film surface (which present uniform Debye rings and for the sake of clarity are shown as diffraction intensity profiles, Figures 2A′ and 3A′), present a well apparent ($\bar{2}10$) reflection, becoming prominent for the co-crystalline phase. As discussed in detail in ref 9a, these diffraction data can be rationalized by the orientation of the *ac* layer of Figure 1 (i.e., of the (010) crystalline planes) preferentially parallel to the film plane (with a degree of parallelism of this plane with respect to the film surface $f_{010} \approx 0.75$). This (010) orientation is shown in Figure 4A, where is indicated as $a_{||}c_{||}$ uniplanar orientation.

X-ray diffraction patterns of s-PS films presenting the nanoporous δ crystalline phase and the intercalate co-crystalline phase with 1,4-dimethyl-naphthalene (DMNP), as obtained by immersion of an α form film in trichloroethylene followed by guest removal and by DMNP sorption, are shown in Figures 2B,B′ and 3B,B′, respectively. In particular, the EDGE patterns present intense (002) reflections on the equatorial line (Figures 2B and 3B) while the THROUGH patterns (Figures 2B′ and 3B′), present a well apparent (010) reflection and the absence of (*hk*2) reflections. As discussed in detail in refs 9b and 10b, these diffraction data can be rationalized by the orientation of the chain axes of the crystalline phases preferentially perpendicular to the film plane (with a degree of parallelism of the 002 plane with respect to the film surface $f_{002} \approx 0.75$). As clearly

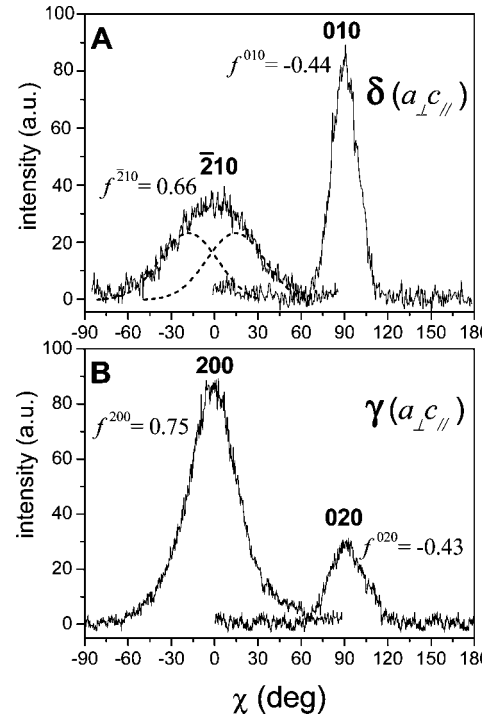

Figure 5. Azimuthal scans relative to the most intense equatorial (χ= 0°) and meridional (χ= 90°) reflections, as collected in EDGE patterns like that one of Figure 2C for: (A) ($\bar{2}10$) and (010) reflections of the nanoporous δ phase, collected at $2\theta_{CuK\alpha}$ =10.2° and 8.4°, respectively; (B) (200) and (020) reflections of the γ phase, collected at $2\theta_{CuK\alpha}$ =9.25° and 10.5°, respectively. The dotted curves of A correspond to the deconvolution of the I(χ) profile of the $\bar{2}10$ reflection.

shown by the molecular model of Figure 4B, this orientation presents the *ac* layers of Figure 1 (i.e., of the (010) crystalline planes) preferentially perpendicular to the film plane. As a consequence, the (002) orientation can be also indicated as $a_{||}$ $c_\perp$ uniplanar orientation.

X-ray diffraction patterns of s-PS films presenting the nanoporous δ crystalline phase and the intercalate co-crystalline phase with 1,4-dimethyl-naphthalene (DMNP), as obtained by immersion of an α form film in chloroform followed by guest removal or by immersion of amorphous film in DMNP, are shown in Figures 2C,C′ and 3C,C′, respectively. In particular, the EDGE patterns present equatorial ($\bar{2}10$) reflections (Figures 2C and 3C) which is particularly intense for the co-crystalline phase[1a] together with a narrow meridional (010) peak, which is particularly intense for the δ phase.[1a] On the other hand, the THROUGH patterns (Figures 2C′ and 3C′), present a well apparent (010) reflection and the presence of (*hk*2) reflections. In ref 10c, analogous diffraction data have been interpreted by the orientation of the ($\bar{2}10$) crystalline plane preferentially parallel to the film plane (with a degree of parallelism with respect to the film surface $f_{\bar{2}10} \approx 0.7$).

In a recent paper,[11] from X-ray diffraction patterns analogous to those of Figures 2C and 3C, and in particular on the basis of the presence of $\bar{2}10$ arcs on the equator being definitely broader than the 010 arcs on the meridian, it has been tentatively suggested that the uniplanar orientation of s-PS, which has been named $\bar{2}10$ orientation, could rather exhibit, as preferentially parallel to the film plane, the crystal plane perpendicular to the *a* axis. This kind of orientation is shown by the model of Figure 4C and can be named as $a_\perp c_{||}$ uniplanar orientation.

Degree of Uniplanar Orientation and $\delta \rightarrow \gamma$ Phase Transition. The main aim of this section is to try to establish if the more recently discovered uniplanar orientation[10c,11] is more correctly described as preferential parallel orientation of

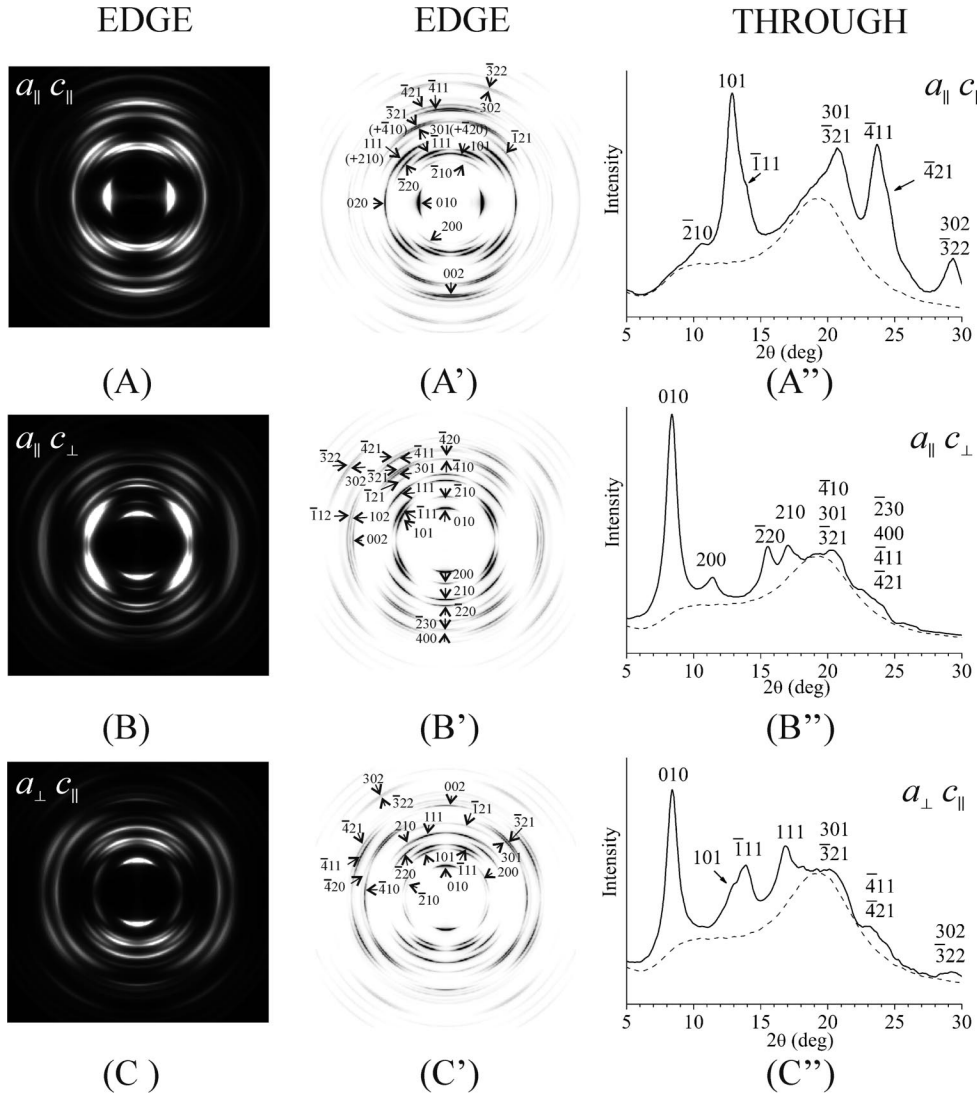

Figure 6. Calculated X-ray diffraction patterns of films of s-PS δ form presenting the indicated uniplanar orientations. A, A″, B, B″, C, C″ allow an immediate comparison with the experimental diffraction patterns reported in Figure 2, parts A, A′, B, B′, C, and C′, respectively. Parts A′, B′, C′ are more schematic representations of A, B, and C patterns to facilitate the indexing of the reflections and a better comparison with the data of Table 1. It is worth noting that the used model of δ form calculates 200 reflection decidedly stronger (by a factor of almost 10) of the $\bar{2}10$ reflection, even if they are both experimentally evaluated very weak.[1a] The X-ray diffraction patterns calculated for the THROUGH images are shown as diffraction intensity profiles to compare with Figure 2A′−C′.

the ($\bar{2}10$) plane or as preferential perpendicular orientation of the (010) plane ($a_{\perp}c_{\parallel}$ uniplanar orientation of Figure 4C), with respect to the film plane. For this purpose, the azimuthal intensity distributions of the main reflections, in EDGE X-ray diffraction patterns like those of Figures 2C and 3C, have been collected and the corresponding orientation functions have been evaluated on the basis of eq 1.

Intensities of the ($\bar{2}10$) and (010) reflections of the nanoporous δ phase (at $2\theta_{\mathrm{CuK}\alpha} = 10.2°$ and 8.4°, respectively) for an EDGE pattern analogous to that one of Figure 2C, are reported versus the azimuthal angle χ in Figure 5A. It is clearly apparent that the equatorial (centered at $\chi = 0°$) ($\bar{2}10$) peak is much broader than the meridional (centered at $\chi = 90°$) (010) peak. On the basis of the $I(\chi)$ distribution of Figure 5A, the degree of perpendicular orientation of the (010) plane is evaluated as $f_{010} \approx -0.44$, i.e. very close to the limit value for complete perpendicular orientation (being - 0.5). On the other hand, the degree of parallel orientation of the ($\bar{2}10$) plane is evaluated as $f_{-210} \approx 0.66$, i.e. rather far from the limit value for complete parallelism (being +1). This suggests that the $I(\chi)$ profile observed for the $\bar{2}10$ reflection is possibly due to the convolution of two narrower peaks centered at $\chi \approx \pm 15°$.

Hence the uniplanar orientation of Figure 2C can be more appropriately rationalized as $a_{\perp}c_{\parallel}$ uniplanar orientation rather than as orientation of the ($\bar{2}10$) plane preferentially parallel to the film plane. In this respect it is worth adding that these two descriptions of the observed orientation are rather similar because a perpendicular to the (010) plane forms an angle of only 17° with respect to the ($\bar{2}10$) plane.

Previous X-ray diffraction studies have shown that, when the monoclinic structures of clathrate[10b] or intercalate[10c] co-crystals as well as that one of the δ phase are transformed (by annealing in the temperature range 120−170°C) into the orthorhombic structure of the γ phase, [9a] the (0k0) uniplanar orientation is maintained while the so called ($\bar{2}10$) orientation is replaced by a (h00) orientation. Figure 5B shows the azimuthal scans as obtained for the EDGE X-ray diffraction pattern of the γ form film obtained by annealing at 160°C of the δ form film of Figure 5A.

By applying the procedure described in eqs1 and 2 of the Experimental Section to the azimuthal scans of the γ form film of Figure 5B, $f_{200} \approx 0.75$ and $f_{020} \approx -0.43$ are obtained. Hence, for the γ phase, as already observed for the δ phase, the degree of perpendicular orientation of the (020) plane is closer to the

Table 1. Comparison between the Relative Intensities of the Reflections of the δ Form Observed in X-ray Diffraction Patterns for Films Exhibiting $a_{\parallel}c_{\parallel}$, $a_{\parallel}c_{\perp}$, and $a_{\perp}c_{\parallel}$ Uniplanar Orientations (Collected with Beams Perpendicular ($\perp$) and Parallel ($\parallel$) to the Film Plane) as Well as for Fibers

	fiber			film $a_{//}c_{//}$				film $a_{//}c_{\perp}$				film $a_{\perp}c_{//}$			
hkl	$2\theta_{obsd}$	$2\theta_{calcd}$	I_{obsd}	I_{obsd} $\perp$	I_{obsd} //	χ_{obsd}	χ_{calcd}	I_{obsd} $\perp$	I_{obsd} //	χ_{obsd}	χ_{calcd}	I_{obsd} $\perp$	I_{obsd} //	χ_{obsd}	χ_{calcd}
010	8.37	8.37	vs		vs	0	0	vs	vs	90	90	vs	vs	90	90
$\bar{2}10$	10.6	10.65	vw	vw	vw	75	73	vw	vw	90	90		ms	10[c]	17
200	11.5	11.41	vw				63				90				27
$\bar{2}20$	15.0	15.43	w		vw	45	41	mw	vvw	90	90		ms	50	49
020	17.0	16.80	w		mw	0	0	mw	vvw	90	90	s[a]	m[a](16.5)	90	90
210		17.00			ms[a]	40	37				90		s(16.5)	55	53
$\bar{4}10$	20.75	20.51	w	ms[b]	m	75	84	mw			90		vs[b]	30	6
$\bar{4}20$		21.41					73				90				17
101	13.35	12.84	vs	ms	m	70	78		vs	30	26	ms	m	65	67
$\bar{1}11$		13.85					65				34				68
111	16.71	16.8	ms		ms[a]	40	49	mw[a]	ms	45	46	s[a]	m[a]	50↔90	72
211	20.7	20.56	s	ms[b]	ms	65	49	mw[b]	s	55	56	ms	vs[b]	30	60
301		20.70					68				56				42
$\bar{3}21$		21.20					65				57				44
$\bar{4}11$	23.5	23.57	s	ms	m	80	85	w	m	60	61	vw	vs	25[c]	30
$\bar{4}21$		24.37					75				62				33
131		30.76		vvw			24				68	vvw	vvw	70	80
002									s	0	0				
102	24.8	23.81	m		vvw	70	84		w	20	14	vw	w	70	78
$\bar{1}12$		24.39					76				19				78
012		24.61					70				20				90
$\bar{2}12$		25.50					83				25				66
202		25.84					78				26				67
112		26.16					65				28				79
212	28.7	28.82	mw	vvw	vvw	70[c]	62		mw	35	36	w	vw	55	69
302		28.92					74				37				58
$\bar{3}22$		29.28					72				38				58
402	33.3	32.79	vw	vvw			71		vvw	40	45	vvw	vvw	50	51
$\bar{3}32$		33.00					58				45				62
432		34.52					64				48				53

[a] Reflections hidden by the more intense first layer-line reflections at $2\theta = 16.71°$. [b] Reflections hidden by the more intense first layer-line reflections at $2\theta = 20.7°$. [c] χ values obtained by peak deconvolution.

limit value than the degree of parallel orientation of the (200) plane.

Moreover, the thermally induced transition from the δ phase toward the γ phase leaves quantitatively unaltered the perpendicular orientation of the *ac* layers (0*k*0 planes) with respect to the film plane while substantially increases the preferential parallel orientation of the (200) planes of the γ phase with respect the orientation of the ($\bar{2}$10) planes of the δ phase. Because an increase of molecular orientation as induced by a thermally activated phase transition is unrealistic, this can be considered as an additional and possibly conclusive indication that the third discovered uniplanar orientation, is not properly described as preferential parallel orientation of the ($\bar{2}$10) planes but should be more accurately interpreted as $a_{\perp}c_{\parallel}$ uniplanar orientation.

In summary, for quantitative evaluations of the degree of $a_{\parallel}c_{\parallel}$ and $a_{\parallel}c_{\perp}$ uniplanar orientations, as proposed in previous reports, the f_{0k0} and f_{00l} orientation functions, i.e., those of the crystal planes preferentially parallel to the film plane, can be used. On the other hand, for the $a_{\perp}c_{\parallel}$ uniplanar orientation, because also for the ideal complete orientation no crystal plane is exactly parallel with respect to the film plane (in fact, for the case of complete $a_{\perp}c_{\parallel}$ uniplanar orientation, the ($\bar{2}$10) planes would form with respect to the film plane an angle of nearly 17°) we propose to use the orientation function f_{0k0}, i.e. a degree of perpendicular orientation, which of course for the case of ideal complete orientation would assume the value $f_{0k0} = -0.5$.

Relative Intensities, Diffraction and Azimuthal Angles of Relevant Bragg Reflections of δ and DMNP Intercalate Phases of s-PS. The 2θ positions and the relative intensities of the reflections of the δ form and of the intercalate phase with DMNP, as observed for the spectra of uniplanar oriented films, like those of Figures 2 and 3, have been collected in Tables 1

Table 2. Comparison between the Relative Intensities of the Reflections of the Intercalate co-Crystalline phase with DMNP Observed in X-ray Diffraction Patterns for Films exhibiting $a_{\parallel}c_{\parallel}$, $a_{\parallel}c_{\perp}$, and $a_{\perp}c_{\parallel}$ Uniplanar Orientations (Collected with Beams Perpendicular (⊥) and Parallel (||) to the Film Plane) as Well as for Fibers

	fiber			film $a_{//}c_{//}$				film $a_{//}c_{\perp}$				film $a_{\perp}c_{//}$			
hkl	$2\theta_{obsd}$	$2\theta_{calcd}$	I_{obsd}	I_{obsd} ⊥	I_{obsd} //	χ_{obsd}	χ_{calcd}	I_{obsd} ⊥	I_{obsd} //	χ_{obsd}	χ_{calcd}	I_{obsd} ⊥	I_{obsd} //	χ_{obsd}	χ_{calcd}
010	5.80	5.74	m		ms	0	0	m	w	90	90	m	w	90	90
$\bar{2}10$	10.05	10.17	s	vs	vs	90	86	vs	s	90	90		vs	0	4
200		11.32					64				90				26
020	11.55	11.51	m		ms	0	0	m	w	90	90	w	vw	90	90
$\bar{2}20$		12.02					57				90		vw (12.1)	35	32
210		14.8		m[a](15)	vs[a](15.3)	45	43	m (14.7)	w (14.7)	90	90	vs[a] (14.9)	s[a] (15.1)	50	47
$\bar{2}30$	15.90	15.9	ms				40	s[a](15.8)	m (15.8)	90	90				50
030		17.2			vw (17.0)	0	0	vw (17.0)	vw (17.0)	90	90		ms (17.0)	90	90
220		19.47					32				90				58
$\bar{4}20$	20.00	20.42	m	ms (20)	m[b] (20.2)	25↔90	86	s[b] (20.2)	vw (20.4)	90	90	mw[b] (20)	ms[b]	40	4
$\bar{2}40$		20.70					29				90				61
$\bar{4}10$		20.85					78				90				13
400	22.60	22.74	mw				64	s[c]	vw	90	90	ms[c]			26
040		23.10			vw(23)	0	0				90		vvw	90	90
101		12.68					79				27				66
011	12.70	12.72	w	vvw	vvw	70	63		vw	25	28	vvw			90
$\bar{1}11$		12.85					65				28				68
111		14.94					56				41				70
$\bar{2}11$		15.25					87				42				48
$\bar{1}21$		15.36					54				42				71
201	15.26	16.06	vs	m[a] (15)	vs[a] (15.3)	45[a]	72	s[a]	vs (15.2)	40	45	vs[a] (14.9)	s[a]	30↔90	51
021		16.17					46				45				90
$\bar{2}21$		16.57					67				47				52
211					s (18.7)	35	55		ms (18.6)	50	53	s (18.5)	m (18.5)	65	57
121		18.72					42				53				74
$\bar{3}11$		18.80													
$\bar{1}31$		19.13					84				53				37
$\bar{3}21$	19.10	19.34	vs	ms (19.1)	m (19.0)	75	40	s (19.1)	ms (19.5)	55	54		19.0	0 ↔ 50	75
$\bar{2}31$		19.47					78				54				38
301		19.60					51				54				59
031		20.51		mw (20.5)	m[b] (20.2)	25 ↔ 90	68	s[b](20.2)	m (20.5)	56	56	mw[b](20.0)	ms[b]	40	42
$\bar{3}31$		20.70					33				57				90
		21.41			w	65	63	vw			58		w	40	44
$\bar{4}21$		23.41		s	s	80[d]	86				61	ms[c]	s	25[d]	29
$\bar{4}11$		23.79					80				61				30
311		23.29					55				61				49
131	23.40	23.47	m				32	s[c]	mw	60	61				77
$\bar{2}41$		23.66					40				61				64
$\bar{1}41$		24.12					31				62				78
$\bar{4}31$		24.45					73				62				73
$\bar{3}41$		24.59					51				62				51
002		22.69					90		vvs (22.6)	0	0				90
112		24.80					70				24				78
$\bar{2}12$		25.01					88				24				66
$\bar{1}22$	25.07	25.08	ms	w	w	30↔90	69		s	25	27	mw	vw	70[d]	78
202		25.52					79				27				66
022		25.60					63				27				90
$\bar{2}22$		25.82					75				28				67
212		27.27					66				33				68
122		27.36					59				33				79
$\bar{3}12$		27.62					86				34				56
$\bar{1}32$		27.79					58				35				79
$\bar{3}22$	27.82	27.79	m	w	w	30↔90	82	vw	w	35	35	vw	vw	65[d]	56
$\bar{2}32$		27.88					64				35				68
302		28.61					75				37				58
032		28.80					53				37				90
$\bar{3}32$		29.28					70				39				58
222		30.19					56				41				70
312		30.72					64				42				60
422		30.83					87				42				48
132	30.50	30.83	w	vvw			50	vvw	vvw	45	42	vvw			80
$\bar{2}42$		30.94					54				42				71
$\bar{4}12$		31.05					82				42				49

[a] Reflections hidden by the more intense first layer-line reflections at $2\theta = 15.26°$. [b] Reflections hidden by the more intense first layer-line reflections at $2\theta = 19.10°$. [c] Reflections hidden by the more intense first layer-line reflections at $2\theta = 23.40°$. [d] χ values obtained by peak deconvolution.

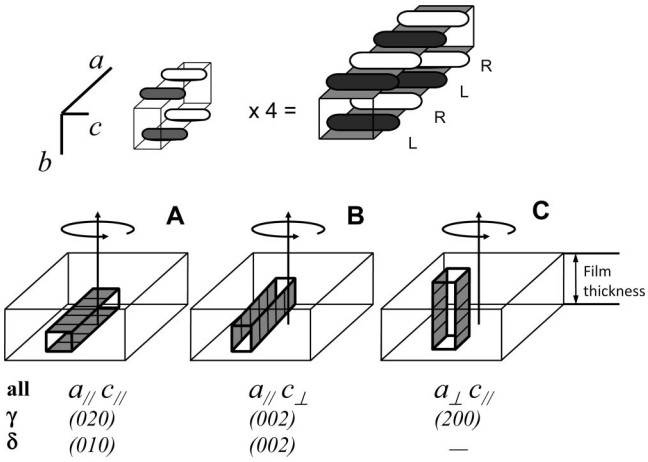

Figure 7. Schematic presentation of the three uniplanar orientations, which can be achieved for helical crystalline (γ and δ) and co-crystalline phases of s-PS. The *ac* layers of alternated enantiomorphous helices can be preferentially parallel (A) or perpendicular to the film plane (B, C). In the models B and C also the *c* and *a* axes are preferentially perpendicular to the film plane. The nomenclatures for the three uniplanar orientations which can be used independently of the crystalline or co-crystalline phases and those which can be used specifically for the γ and δ phases are also shown in the bottom of the figure.

and 2, respectively. For the sake of comparison, Table 1 and Table 2 also report the information obtained by X-ray diffraction patterns of corresponding uniaxially stretched films, as well as the Miller indexes of the reflections, as derived by the crystal structures of refs 1a and 7d, respectively.

As for the EDGE patterns of the uniplanar oriented films, Tables 1 and 2 also report the azimuthal angles χ_{obs} corresponding to the maximum intensity of the observed arc reflections. Both Tables also report the calculated azimuthal angles χ_{calc}, where the reflection should be observed for the case of limit complete $a_{||}c_{||}$, $a_{||}c_{\perp}$ and $a_{\perp}c_{||}$ uniplanar orientations.

The rather good agreement between the observed and calculated azimuthal angles confirms that the three proposed orientations well represent those obtained for s-PS films.

In order to allow a more immediate comparison between observed and calculated data we have calculated, for the case of δ form, on the basis of the literature model, [1a] the EDGE and THROUGH X-ray diffraction patterns for films presenting the three discussed uniplanar orientations (Figure 6).

The data reported in Tables 1 and 2 also show that X-ray diffraction patterns of films presenting the different uniplanar orientation allow a separation between Bragg reflections, which cannot been separated in X-ray diffraction patterns of uniaxially oriented samples. For instance, for the δ form, the 020 and 210 reflections can be easily separated in EDGE X-ray diffraction patterns of films presenting the $a_{||}c_{||}$ and $a_{\perp}c_{||}$ orientations, because they appear at completely different azimuthal χ angles (see 7th and 15th columns of Table 1).

It is also worth adding that the azimuthal angles observed for the *hk*1 peak at $2\theta \approx 23.4°$ of the DMNP co-crystalline films with $a_{||}$ $c_{||}$ and $a_{\perp}$ $c_{||}$ orientations (χ_{obs} of 7th and 15th columns of Table 2) allow to establish that $\bar{4}21$ and $\bar{4}11$ reflections mostly contribute to this peak while the contributions of the 311, 131, $\bar{2}41$, $\bar{1}41$, $\bar{4}31$, $\bar{3}41$ are nearly negligible.

Schematic Presentation of the Three Uniplanar Orientations. A schematic presentation of the three uniplanar orientations, which can be achieved for helical crystalline (γ and δ) and co-crystalline phases of s-PS by suitable crystallization procedures, corresponding to the more detailed molecular models of Figure 4, are shown in Figure 7.

The unit cell (and unit cell axes) of the s-PS crystalline (or co-crystalline phase) is schematically shown in the upper left part of Figure 7. A model formed by only two *ac* layers, which schematically represents an exaggeratedly small crystallite, is presented in the upper right part Figure 7. The three possible orientations of this crystallite (and hence of the *ac* layers) with respect to the film plane, previously shown by molecular models in Figures 4A−C, are shown in Figures 7A−C, respectively. The arrows added on the models of Figures 7A−C remind that there is a lack of axial orientation.

Independently of the crystalline (γ and δ) or co-crystalline phases of s-PS, the three uniplanar orientations schematized in Figure 7, parts A, B, and C, can be named $a_{||}c_{||}$, $a_{||}c_{\perp}$, and $a_{\perp}c_{||}$ uniplanar orientations.

These three orientations for the case of the orthorhombic γ phase correspond to (020), (002) and (200) crystalline planes preferentially parallel to the film plane. On the other hand for the monoclinic δ and co-crystalline phases, the first two uniplanar orientations correspond to the (010) and (002) crystalline planes preferentially parallel to the film plane while for the $a_{\perp}c_{||}$ uniplanar orientation no relevant crystalline plane is precisely parallel to the film plane.

These considerations also indicate that, for the sake of clarity, it would be helpful to prefer for s-PS films the presently proposed nomenclature of $a_{||}c_{||}$, $a_{||}c_{\perp}$, and $a_{\perp}c_{||}$ uniplanar orientations.

X-ray Diffraction Patterns, Taken with an Automatic Powder Diffractometer, of Films Presenting Uniplanar Orientations of Their Crystalline Phases. In this final section, X-ray diffraction patterns of films presenting the three different kinds of uniplanar orientations of the nanoporous δ phase and of the intercalate phase with DMNP and of the γ phase, as collected by an automatic powder diffractometer, i.e., with the technique most frequently used in the majority of laboratories, are compared.

The main aim is to facilitate the recognition of the possible occurrence and of the kind of uniplanar orientation in s-PS samples, by using simple and rapidly achieved diffraction measurements.

The X-ray diffraction patterns shown in Figure 8 A−C, correspond to the δ form of films of Figure 2A−C, respectively, while those shown in Figure 8 A′−C′ correspond to the intercalate s-PS/DMNP films of Figure 3A−C, respectively. The X-ray diffraction patterns shown in Figure 8 A″−C″, correspond to the γ films obtained by annealing at 160°C of the δ form films of Figure 8A−C. For the sake of comparison, the X-ray diffraction patterns of unoriented δ, s-PS/DMNP and γ form powder samples are shown in Figure 8, parts D, D′, and D″, respectively.

Generally, a high intensity of the (010) reflection, located at $d = 1.05$ nm ($2\theta_{CuK\alpha} = 8.4°$) for the δ phase and shifted up to $d = 1.6-1.8$ nm ($5° < 2\theta_{CuK\alpha} < 8.4°$) for the co-crystalline phases, clearly indicates the occurrence of the $a_{||}c_{||}$ uniplanar orientation. As for γ form samples the $a_{||}c_{||}$ uniplanar orientation corresponds to an intense (020) reflection located at $d = 0.84$ nm ($2\theta_{CuK\alpha} = 10.5°$, Figure 8A″).

A high intensity of the (002) reflection, located close to $d = 0.39$ nm ($2\theta_{CuK\alpha} = 22.5°$), independently of the helical crystalline or co-crystalline phase, clearly indicates the occurrence of the $a_{||}c_{\perp}$ uniplanar orientation.

Finally, the occurrence of the $a_{\perp}c_{||}$ uniplanar orientation can be easily recognized for s-PS co-crystalline phases by the presence of a very intense ($\bar{2}10$) peak, generally located in the range $10° < 2\theta_{CuK\alpha} < 10.7°$ (Figure 8C′) or for the γ phase by the presence of a very intense (200) peak, located at $d = 0.96$ nm ($2\theta_{CuK\alpha} = 9.25°$, Figure 8C″).

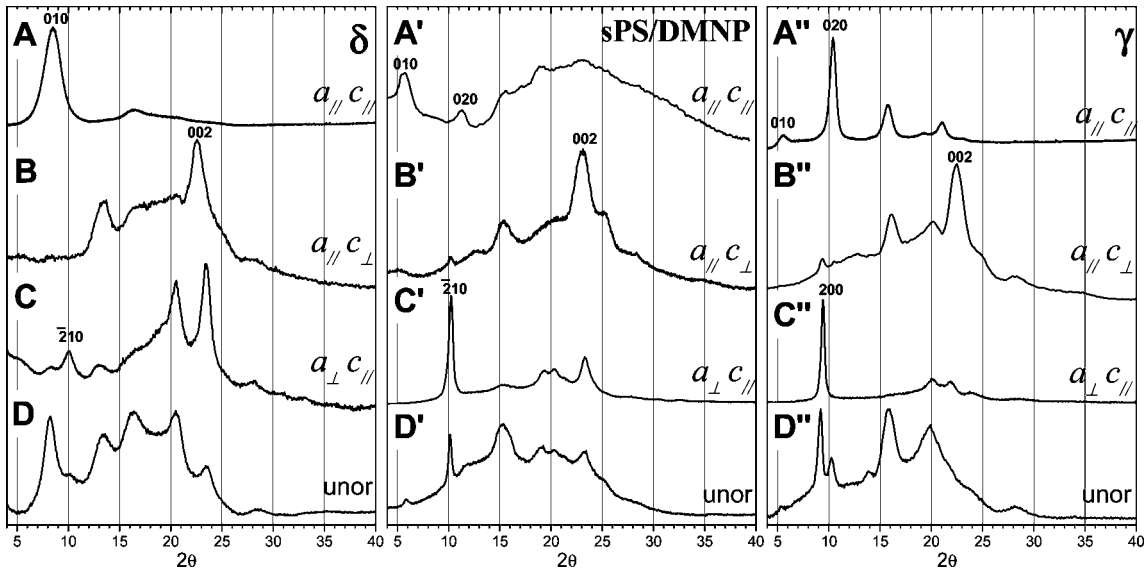

Figure 8. X-ray diffraction patterns of unoriented and uniplanar oriented s-PS samples, as collected by an automatic powder diffractometer, exhibiting the δ (A−D), s-PS/DMNP intercalate (A′−D′) and γ (A″−D″) phases: films presenting $a_{||}c_{||}$ (A), $a_{||}c_{\perp}$ (B), and $a_{\perp}c_{||}$ (C) uniplanar orientations and powders (D)

.

The occurrence of the $a_{\perp}c_{||}$ uniplanar orientation for the δ phase, also maximizes the intensity of the ($\bar{2}$10) peak, located at $d = 0.834$ nm ($2\theta_{CuK\alpha} = 10.6°$, Figure 8C) although, due to the intrinsic weakness of the ($\bar{2}$10) reflection of the nanoporous δ phase,[1a] this peak does not become prominent. However, the occurrence of the $a_{\perp}c_{||}$ uniplanar orientation can be assumed for the δ phase when the ($\bar{2}$10) peak becomes more intense than the (010) peak (Figure 8C), which is instead one of the most intense reflections of this nanoporous phase.

***a*−*c* Layers and Mechanism of Formation of the Three Different Uniplanar Orientations of s-PS Films.** The X-ray diffraction analyses of the previous sections, have allowed concluding that the three uniplanar orientations observed for s-PS films correspond to the three simplest orientations of the high planar-density *ac* layers, with respect to the film plane. This conclusion, associated with experimental co-crystallization data reported in previous papers,[9−11] contributes to a definition of possible mechanisms leading to the different kinds of uniplanar orientations for different co-crystallization procedures.

For biaxial stretching, only the $a_{||}c_{||}$ uniplanar orientation has been observed.[10a] This observation can be easily rationalized, because for hydrocarbon polymers (for which the only interchain interactions are of Van der Waals type) the primary slip plane, i.e., the plane which tends to become parallel to the film surface, is generally that one containing the chain axis and having the highest density.[21]

As for solution casting procedures,[9] the two alternative uniplanar orientations ($a_{||}c_{||}$ and $a_{||}c_{\perp}$) are determined by the chemical nature of the solvent (that also becomes the guest of the polymer co-crystalline phases) which, in turn, mainly influences the correlation length perpendicular to the ac layers (4 nm < D_{010} < 14 nm), while the guest influence for correlation length along other crystalline directions is generally poor.[9c] In particular, $a_{||}c_{||}$ uniplanar orientation occurs with guests exhibiting poor host-guest interactions,[22] corresponding to low crystal-growth rates perpendicular to the *ac* layers and leading to low D_{010} values (4nm < D_{010} < 6 nm).[9c] On the other hand, $a_{||}c_{\perp}$ uniplanar orientation occurs for guests exhibiting good host−guest interactions[22] corresponding to high crystal-growth rates perpendicular to the *ac* layers and leading to high D_{010} values (7 nm < D_{010} < 16 nm).[9c] In the latter case, the crystal-growth rate would become minimum along the chain-axis, thus leading to the observed orientation with *c*-axes perpendicular to the film plane.

As for solvent-induced crystallization in s-PS amorphous films,[11] the two alternative uniplanar orientations ($a_{||}c_{\perp}$ and $a_{\perp}c_{||}$) are essentially only determined by the guest volatility. In fact, more volatile guests (boiling point [bp] < 120 °C or vapor pressure [vp] > 20 Torr) induce $a_{||}c_{\perp}$ uniplanar orientation while less volatile guests (bp > 140 °C or vp < 7 Torr) induce $a_{\perp}c_{||}$ uniplanar orientation (Table 1 of ref 11), independent of other chemical or structural features of the guest. This indicates that, when the rate of advancement of the guest front is fast (and hence is not a rate-determining-step for crystallization), the crystal growth occurs with *c* axes perpendicular to the advancing front (and film surface); i.e., the speed of crystal growth along the *c*-axis direction is expected to be the lowest. On the other hand, when the rate of advancement of the guest front is low, thus possibly becoming the rate-determining-step for the crystallization process, a sort of two dimensional confinement of the co-crystallization process occurs, favoring the orientation of the polymer chains parallel to the film surface and crystal growths with a axes perpendicular to the advancing front. It is worth adding, that the $a_{||}c_{||}$ uniplanar orientation, although the most common for s-PS co-crystalline films, has never been obtained by solvent induced crystallization or re-crystallization procedures (for a collection of data see the last three columns of Table 1 of ref 11). This could be possibly related to the minimum guest diffusivities which have been calculated and observed perpendicular to the *ac* planes.[18]

Conclusions

The main conclusion of this paper is that the layer of close-packed alternated enantiomorphous helices that characterizes the δ phase of s-PS, as well as all related clathrate and intercalate co-crystalline phases with low-molecular-mass guest molecules, is the structural feature determining the three different uniplanar orientations, which have been obtained for γ, δ and co-crystalline s-PS phases.

In fact, thorough analyses of X-ray diffraction patterns of s-PS films exhibiting different crystalline and co-crystalline phases, and related evaluations of degrees of orientation, have

allowed to conclude that the three observed uniplanar orientations correspond to the three simplest orientations of the high planar-density *ac* layers, i.e. of close-packed alternated enantiomorphous s-PS helices, with respect to the film plane.

In particular, it has been established that the uniplanar orientation, formerly defined as preferential parallel orientation of the $(\bar{2}10)$ crystal plane with respect to the film plane, has to be more properly defined as the orientation of the *ac* plane perpendicular to the film plane, with the *c* axis parallel and the *a* axis perpendicular to the film plane.

On this basis it is proposed that the three uniplanar orientations of s-PS should be preferably named $a_{||}c_{||}$, $a_{||}c_{\perp}$ and $a_{\perp}c_{||}$. The presently proposed nomenclature presents the additional advantage that can be used unaltered for both γ and δ crystalline phases as well as for co-crystalline phases of s-PS.

For quantitative evaluations of the of $a_{||}c_{||}$ and $a_{||}c_{\perp}$ uniplanar orientations the f_{0k0} and f_{00l} orientation functions, i.e. those evaluated on the basis of the azimuthal intensity distribution of the reflections corresponding to the crystal planes preferentially parallel to the film plane, are used. The cases of ideal complete $a_{||}c_{||}$ and $a_{||}c_{\perp}$ orientations would correspond to $f_{0k0} = 1$ and $f_{00l} = 1$, respectively. On the other hand, for the $a_{\perp}c_{||}$ uniplanar orientation, because also for the ideal complete orientation no crystal plane is exactly parallel with respect to the film plane, it is proposed the use of the orientation function f_{0k0}, i.e., a degree of perpendicular orientation, which for the case of ideal complete orientation would assume the value $f_{0k0} = -0.5$.

X-ray diffraction patterns of γ, δ, and s-PS/DMNP co-crystalline films presenting the three different kinds of uniplanar orientations, as collected by an automatic powder diffractometer, have been compared with the spectra of the corresponding unoriented samples. The reported patterns will facilitate the recognition of the possible occurrence and of the kind of uniplanar orientation in s-PS films, by simply using an automatic powder diffractometer.

The paper also shows (Tables 1 and 2) that EDGE X-ray diffraction patterns of films presenting the three different uniplanar orientation allows a separation between some Bragg reflections, which are not separated in X-ray diffraction patterns of uniaxially oriented samples.

Acknowledgment. The authors thank Prof. Vincenzo Venditto of the University of Salerno for useful discussions. Financial support of the "Ministero dell'Istruzione, dell'Università e della Ricerca" (PRIN 2007) and of "Regione Campania" (Centro di Competenza per le Attività Produttive) is gratefully acknowledged.

References and Notes

(1) (a) De Rosa, C.; Guerra, G.; Petraccone, V.; Pirozzi, B. *Macromolecules* **1997**, *30*, 4147. (b) Reverchon, E.; Guerra, G.; Venditto, V. *J. Appl. Polym. Sci.* **1999**, *74*, 2077. (c) Milano, G.; Venditto, V.; Guerra, G.; Cavallo, L.; Ciambelli, P.; Sannino, D *Chem. Mater.* **2001**, *13*, 1506. (d) Sivakumar, M.; Mahesh, K. P. O.; Yamamoto, Y.; Yoshimizu, H.; Tsujita, Y. *J. Polym. Sci., Polym. Phys.* **2005**, *43*, 1873. (e) Gowd, E. B.; Shibayama, N.; Tashiro, K. *Macromolecules* **2006**, *39*, 8412.

(2) (a) Rizzo, P.; Daniel, C.; De Girolamo Del Mauro, A; Guerra, G. *Chem. Mater.* **2007**, *19*, 3864. (b) Rizzo, P.; D'Aniello, C.; De Girolamo Del Mauro, A.; Guerra, G. *Macromolecules* **2007**, *40*, 9470. (c) Petraccone, V.; Ruiz de Ballesteros, O.; Tarallo, O.; Rizzo, P.; Guerra, G. *Chem. Mater.* **2008**, *20*, 3663.

(3) (a) Manfredi, C.; Del Nobile, M. A.; Mensitieri, G.; Guerra, G.; Rapacciuolo, M. *J. Polym. Sci., Polym. Phys. Ed.* **1997**, *35*, 133. (b) Guerra, G.; Manfredi, C.; Musto, P.; Tavone, S. *Macromolecules* **1998**, *31*, 1329. (c) Musto, P.; Manzari, M.; Guerra, G. *Macromolecules* **2000**, *33*, 143. (d) Musto, P.; Mensitieri, G.; Cotugno, S.; Guerra, G.; Venditto, V. *Macromolecules* **2002**, *35*, 2296. (e) Saitoh, A.; Amutharani, D.; Yamamoto, Y.; Tsujita, Y.; Yoshimizu, H. *Desalination* **2002**, *148*, 353. (f) Larobina, D.; Sanguigno, L.; Venditto, V.; Guerra, G.; Mensitieri, G. *Polymer* **2004**, *45*, 429. (g) Mahesh, K.P.O.; Sivakumar, M; Yamamoto, Y; Tsujita, Y.; Yoshimizu, H.; Okamoto, S. *J. Membrane Sci.* **2005**, *262*, 11. (h) Mensitieri, G.; Larobina, D.; Guerra, G.; Venditto, V.; Fermeglia, M.; Pricl, S. *J. Polym. Sci., Part B: Polym. Phys.* **2008**, *46*, 8.

(4) (a) Daniel, C.; Alfano, D.; Venditto, V.; Cardea, S.; Reverchon, E.; Larobina, D.; Mensitieri, G.; Guerra, G. *Adv. Mater.* **2005**, *17*, 1515. (b) Malik, S.; Roizard, D.; Guenet, J. M. *Macromolecules,* **2006**, *39*, 5957. (c) Daniel, C.; Sannino, D.; Guerra, G. *Chem. Mater.* **2008**, *20*, 577.

(5) (a) Mensitieri, G.; Venditto, V.; Guerra, G. *Sens. Actuators, B* **2003**, *92*, 255. (b) Giordano, M.; Russo, M.; Cusano, A.; Cutolo, A.; Mensitieri, G.; Nicolais, L. *Appl. Phys. Lett.* **2004**, *85*, 92. (c) Cusano, A.; Pilla, P.; Contessa, L.; Iadicicco, A.; Campopiano, S.; Cutolo, A.; Giordano, M.; Guerra, G. *Appl. Phys. Lett.* **2005**, *87*, 234105. (d) Giordano, M.; Russo, M.; Cusano, A.; Mensitieri, G.; Guerra, G. *Sens. Actuators, B* **2005**, *109*, 177. (e) Cusano, A.; Iadicicco, A.; Pilla, P.; Contessa, L.; Campopiano, S.; Cutolo, A.; Giordano, M.; Guerra, G. *J. Lightwave Tech.* **2006**, *24*, 1776. (f) Buono, A.; Rizzo, P.; Immediata, I.; Guerra, G. *J. Am. Chem. Soc.* **2007**, *129*, 10992. (g) Guadagno, L.; Raimondo, M.; Silvestre, C.; Immediata, I.; Rizzo, P.; Guerra, G. *J. Mater. Chem.* **2008**, *18*, 567.

(6) (a) Chatani, Y.; Inagaki, T.; Shimane, Y.; Ijitsu, T.; Yukimori, T.; Shikuma, H. *Polymer* **1993**, *34*, 1620. (b) Chatani, Y.; Shimane, Y.; Inagaki, T. Shikuma, H. *Polymer* **1993**, *34*, 4841. (c) De Rosa, C.; Rizzo, P.; Ruiz de Ballesteros, O.; Petraccone, V.; Guerra, G *Polymer* **1999**, *40*, 2103. (d) Tarallo, O.; Petraccone, V. *Macromol. Chem. Phys.* **2004**, *205*, 1351. (e) Tarallo, O.; Petraccone, V. *Macromol. Chem. Phys.* **2005**, *206*, 672.

(7) (a) Rastogi, S.; Goossens, J. G. P.; Lemstra, P. J. *Macromolecules* **1998**, *31*, 2983. (b) van Hooy-Corstjens, C. S. J.; Magusin, P. C. M. M.; Rastogi, S.; Lemstra, P. J. *Macromolecules* **2002**, *35*, 6630. (c) Petraccone, V.; Tarallo, O.; Venditto, V.; Guerra, G. *Macromolecules* **2005**, *38*, 6965. (d) Tarallo, O.; Petraccone, V.; Venditto, V.; Guerra, G. *Polymer* **2006**, *47*, 2402. (e) Malik, S.; Rochas, C.; Guenet, J.-M. *Macromolecules* **2006**, *39*, 1000. (f) Galdi, N.; Albunia, A. R.; Oliva, L.; Guerra, G. *Macromolecules* **2006**, *39*, 9171.

(8) (a) Venditto, V.; Milano, G.; De Girolamo Del Mauro, A.; Guerra, G.; Mochizuki, J.; Itagaki, H. *Macromolecules* **2005**, *38*, 3696. (b) Stegmaier, P.; De Girolamo Del Mauro, A.; Venditto, V.; Guerra, G. *Adv.Mater.* **2005**, *17*, 1166. (c) Uda, Y.; Kaneko, F.; Tanigaki, N.; Kawaguchi, T. *Adv. Mater.* **2005**, *17*, 1846. (d) Kaneko, F.; Uda, Y.; Kajiwara, A.; Tanigaki, N. *Macromol.Rapid Commun* **2006**, *27*, 1643. (e) D'Aniello, C.; Musto, P.; Venditto, V.; Guerra, G. *J. Mater. Chem.* **2007**, *17*, 531. (f) Daniel, C.; Galdi, N.; Montefusco, T.; Guerra, G. *Chem. Mater.* **2007**, *19*, 3302. (g) De Girolamo Del Mauro, A.; Carotenuto, M.; Venditto, V.; Petraccone, V.; Scoponi, M.; Guerra, G. *Chem. Mater.* **2007**, *19*, 6041.

(9) (a) Rizzo, P.; Lamberti, M.; Albunia, A. R.; Ruiz de Ballesteros, O.; Guerra, G. *Macromolecules* **2002**, *35*, 5854. (b) Rizzo, P.; Costabile, A.; Guerra, G. *Macromolecules* **2004**, *37*, 3071. (c) Daniel, C.; Avallone, A.; Rizzo, P.; Guerra, G. *Macromolecules* **2006**, *39*, 4820.

(10) (a) Rizzo, P.; Albunia, A. R.; Milano, G.; Venditto, V.; Guerra, G.; Mensitieri, G.; Di Maio, L. *Macromol. Symp.* **2002**, *185*, 65. (b) Rizzo, P.; Della Guardia, S.; Guerra, G. *Macromolecules* **2004**, *37*, 8043. (c) Rizzo, P.; Spatola, A.; De Girolamo Del Mauro, A.; Guerra, G. *Macromolecules* **2005**, *38*, 10089.

(11) Albunia, A. R.; Annunziata, L.; Guerra, G. *Macromolecules* **2008**, *41*, 2683.

(12) (a) Immirzi, A.; de Candia, F.; Iannelli, P.; Zambelli, A.; Vittoria, V. *Makromol. Chem., Rapid Commun.* **1988**, *9*, 761. (b) Tamai, Y.; Fukuda, M. *Macromol. Rapid Commun.* **2002**, *23*, 892. (c) Rizzo, P.; Albunia, A. R.; Guerra, G. *Polymer* **2005**, *46*, 9549.

(13) (a) Chatani, Y.; Shimane, Y.; Inoue, Y.; Inagaki, T.; Ishioka, T.; Ijitsu, T.; Yukinari, T. *Polymer* **1993**, *33*, 488. (b) Yoshioka, A.; Tashiro, K. *Macromolecules* **2003**, *36*, 3593. (c) Uda, Y.; Kaneko, F.; Kawaguchi, T. *Polymer* **2004**, *45*, 2221. (d) Uda, Y.; Kaneko, F.; Kawaguchi, T. *Macromolecules* **2005**, *38*, 3380. (e) Tashiro, K. *Macromol. Symp.* **2005**, *222*, 115.

(14) (a) Guerra, G.; Vitagliano, V. M.; De Rosa, C.; Petraccone, V.; Corradini, P. *Macromolecules* **1990**, *23*, 1539. (b) De Rosa, C.; Guerra, G.; Petraccone, V.; Corradini, P *Polym. J.* **1991**, *23*, 1435. (c) De Rosa, C. *Macromolecules* **1996**, *29*, 8460. (d) Cartier, L.; Okihara, T.; Lotz, B. *Macromolecules* **1998**, *31*, 3303.

(15) (a) De Rosa, C.; Rapacciuolo, M.; Guerra, G.; Petraccone, V.; Corradini, P. *Polymer* **1992**, *33*, 1423. (b) Chatani, Y.; Shimane, Y.; Ijitsu, T.; Yukinari, T. *Polymer* **1993**, *34*, 1625.

(16) Albunia, A. R.; Rizzo, P.; Guerra, G.; Torres, F. J.; Civalleri, B.; Zicovich-Wilson, C. M. *Macromolecules* **2007**, *40*, 3895.

(17) (a) Albunia, A. R.; Di Masi, S.; Rizzo, P.; Milano, G.; Musto, P.; Guerra, G. *Macromolecules* **2003**, *36*, 8695. (b) Albunia, A. R.; Milano, G.; Venditto, V.; Guerra, G *J. Am. Chem. Soc.* **2005**, *127*, 13114.

(18) (a) Milano, G.; Guerra, G.; Müller-Plathe, F. *Chem. Mater.* **2002**, *14*, 2977. (b) Venditto, V.; De Girolamo Del Mauro, A.; Mensitieri, G.;

Milano, G.; Musto, P.; Rizzo, P.; Guerra, G. *Chem. Mater.* **2006**, *18*, 2205. (c) Annunziata, L.; Albunia, A. R.; Venditto, V.; Guerra, G. *Macromolecules* **2006**, *39*, 9166. (d) Albunia, A. R.; Minucci, T.; Guerra, G. *J. Mater. Chem.* **2008**, *18*, 1046.

(19) Albunia, A.R.; Musto, P.; Guerra, G. *Polymer* **2006**, *47*, 234.

(20) (a) Wilchinsky, Z. W. *Advances in X-ray analysis*; Plenum Press: New York, 1963; Vol. *6*, p 231. (b) Alexander, L. E. In *X-Ray Diffraction Methods in Polymer Science*; Krieger, R. E., Ed.; Hundington: New York, 1979; Chapter 4, p 210.

(21) (a) Heffelfinger; Burton, R. L. *J. Polym. Sci.* **1960**, *47*, 289. (b) Werner, E.; Janocha, S.; Hopper, M. J. *Mackenzie Encyclopedia of Polymer Science and Engineering*; 2nd ed.; Wiley-Interscience: New York, 1986; Vol. *12*; p 193. (c) Gohil, R. M. *J. Appl. Polym. Sci.* **1993**, *48*, 1649. (d) Uejo, H.; Hoshino, S. *J. Appl. Polym. Sci.* **1970**, *14*, 317. (e) Rizzo, P.; Venditto, V.; Guerra, G.; Vecchione, A. *Macromol. Symp.* **2002**, *185*, 53.

(22) Daniel, C.; Avallone, A.; Guerra, G. *Macromolecules* **2006**, *39*, 7578.

MA801180B